



# Direct cyber-power interdependencies-based reliability evaluation of smart grids including wind/solar/diesel distributed generations and plug-in hybrid electrical vehicles



Hamed Hashemi-Dezaki<sup>a,\*</sup>, Hossein Askarian-Abyaneh<sup>b</sup>, Amirhasan Shams-Ansari<sup>c</sup>,  
Mohammad DehghaniSanij<sup>d</sup>, Maryam A. Hejazi<sup>a</sup>

<sup>a</sup> Department of Electrical and Computer Engineering, University of Kashan, 6 km Ghotbravandi Blvd, postal code: 8731753153, Kashan, Iran

<sup>b</sup> Department of Electrical Engineering, Amirkabir University of Technology (Tehran Polytechnic), Power System Excellence, Tehran 15914, Iran

<sup>c</sup> Department of Electrical and Computer Engineering, Howard University, Washington, D.C., United States

<sup>d</sup> Department of Electrical Engineering, Ashkezar Branch, Islamic Azad University, Ashkezar, Iran

## ARTICLE INFO

### Article history:

Received 24 October 2016

Received in revised form 4 February 2017

Accepted 17 May 2017

### Keywords:

Smart grid

Direct cyber-power interdependencies (DCPIs)

Plug-in hybrid electric vehicles (PHEVs)

Monte Carlo simulation (MCS)

Reliability evaluation

Uncertainty

## ABSTRACT

Smart grid is a so-called “cyber-power system” because the cyber systems (control/monitoring/protection, and communication networks) are integrated to power systems in it. The less effort has been devoted in literature to reliability evaluation based on direct cyber-power Interdependencies (DCPIs) in widespread presence of distributed generations (DGs) and charging load of plug-in hybrid electric vehicles (PHEVs) as supply side uncertainties and demand side ones. The consideration of uncertainty regarding the PHEVs in addition to other uncertain aspects inside the DCPIs is one of the most important contributions of this paper. In addition, the sensitivity analysis of reliability versus the variation of failures in power and cyber elements is essentially analyzed. The introduced method is applied to two realistic case studies. The test results infer that the DCPI-based reliability evaluation of smart grids including DGs and PHEVs is achievable through use of the proposed method. Because of using the Monte Carlo simulation (MCS), it is possible to extend the proposed method by integration of future uncertain and stochastic subjects without any limit. Further, the test results illustrate that the communication failures as direct network-element interdependencies (DNEI) is more important than direct element-element interdependencies (DEEI). The numerical results also imply that the risk level due to DCPIs increases due to inappropriate cyber network configurations.

© 2017 Elsevier Ltd. All rights reserved.

## 1. Introduction

The integration of control, monitoring, protection, information, and communication infrastructures to power network leads to create a so-called “cyber-power system”. The power and cyber networks of smart grid are governed by their own different laws, protocols, and characteristics [1–3]. The literature on the modernized power systems reliability examining the cyber elements is numerable [4]. Singh and Sprintson [4] focused on the reliability assurance of cyber-physical systems, and introduced a novel classification of cyber failures. It should be noted that the reliabil-

ity evaluation of cyber-physical systems based on mutual cyber-power interdependencies is an interesting subject.

In addition to smart grid and power systems, the reliability evaluation of heterogeneous cyber-physical system has attracted a lot of attentions. L. Zhang, et al. [5] introduced a method for improving the energy efficiency and system reliability for precedence constrained tasks in heterogeneous systems. The reliability optimization with energy conservation for parallel task scheduling in a heterogeneous cluster was focused in [6]. K. Li et al. [7] in heterogeneous cluster systems studied the scheduling precedence based on constrained stochastic tasks. These researches illustrate the importance of reliability evaluation of cyber-physical and heterogeneous systems. The cyber networks may adversely affect the modernized power system, and the power and energy systems may adversely affect the reliability of computing systems. Therefore, developing the novel reliability evaluation method based on

\* Corresponding author.

E-mail addresses: [hamed.hashemi@aut.ac.ir](mailto:hamed.hashemi@aut.ac.ir) (H. Hashemi-Dezaki), [askarian@aut.ac.ir](mailto:askarian@aut.ac.ir) (H. Askarian-Abyaneh), [amirhasan.shams@bison.howard.edu](mailto:amirhasan.shams@bison.howard.edu) (A. Shams-Ansari), [Mohammad.d@aut.ac.ir](mailto:Mohammad.d@aut.ac.ir) (M. DehghaniSanij), [mhejazi@kashanu.ac.ir](mailto:mhejazi@kashanu.ac.ir) (M.A. Hejazi).

## Nomenclature

$v, V$	wind speed (m/s)	$N_{SR}, N_{seg}, C, K, n_{bus}$	total number of servers, segments, operation modes, system elements, and buses
$F(V)$	Weibull cumulative density function (CDF) of wind speed	$HS_m, MS_m, RS_m$	healthy, marginal, and at-risk period of $m$ -th iteration of MCS
$k, c$	shape and scale parameters of Weibull CDF	$R_{cons}^n, R_{chg}^n$	electric energy consumption (kWh/km) and electric charging rate of $n$ -th PHEV (kW)
$\sigma$	standard deviation	$\Delta x(t, n), \Delta t(t, n)$	travelled distance and charging time of $n$ -th PHEV in $t$ -th time segment
$v_m$	mean wind speed (m/s)	$\sigma_{PHEV\_ETD}, \sigma_{PHEV\_MTD}$	standard deviation values of PHEV evening and morning traveling distance
$f(v), f(k_t)$	probability density function (pdf) of wind speed and clearness index	$\mu_{PHEV\_ETD}, \mu_{PHEV\_MTD}$	mean values of PHEV evening and morning traveling distance
$u$	random number uniformly distributed on [01]	$\sigma_{PHEV\_AT}, \sigma_{PHEV\_DT}$	standard deviation values of PHEV arrival and departure times
$P_W(v), P_{rated}$	output power of wind turbine (W) and rated output power of wind turbine (W)	$\mu_{PHEV\_AT}, \mu_{PHEV\_DT}$	mean values of PHEV arrival and departure times
$v_{ci}, v_{rated}, v_{co}$	cut-in, rated, and cut-off speed of wind turbine (m/s)	$AT(n), DT(n)$	arrival time and departure time of $n$ -th PHEV
$K_t, \bar{K}_t$	instantaneous and mean value of hourly clearness index	$Availability(j, t)$	availability and unavailability of $j$ -th element in the $t$ -th time segment
$G, G_0$	irradiance on a horizontal plane and extraterrestrial total solar irradiance (kW/m <sup>2</sup> )	$S(t), S'(t), S''(t)$	state vector of system in $t$ -th time segment during ordinary (direct network-element interdependencies) DNEI, and (direct element-element interdependencies) DEEI mapped conditions
$\alpha, \beta$	position and shape parameter of Beta probability distribution	$S(t, i), S'(t, i), S''(t, i)$	the $i$ -th element of state vector in the $t$ -th time segment during ordinary, DNEI, and DEEI mapped conditions
$\sigma_{k_t}$	standard deviation of clearness index	$DNEL(j, i)$	binary element of direct network-element link (DNEL) matrix corresponding to the DNEI between the $j$ -th cyber element and the $i$ -th power one
$T_c, T_a$	solar cell and ambient temperature (°C)	$P_G, P_{DDG}, P_{G, DG_s}$	total power generation, output power of dispatchable DG units, and output power of all DG units
$N_{OT}$	nominal operating temperature of the solar cell (°C)	$P_{Loads}, P_{MainSub}, P_{Loss}$	demand load, power provided by main 63/20 kV substation, and active power loss
$I$	output current of the photo voltaic modules (A)	$V_{t,i}, \delta_{t,j}$	voltage magnitude and phase angle of the $i$ -th bus in the $t$ -th time
$I_{sc}$	short circuit current of photovoltaic modules (A)	$Y_{ij}, \theta_{ij}$	magnitude and phase angle regarding the element of admittance matrix corresponding to the $i$ -th row and $j$ -th column
$K_I$	current temperature coefficient (A/°C)	$P_l, P_{max,l}$	power passing through the $l$ -th distribution line and the power limit of $i$ -th line
$V, V_{oc}$	output voltage and open circuit voltage of photovoltaic modules (V)	$K_{D2T}$	ratio of power generation of dispatchable DGs to all DG units
$k_V$	voltage temperature coefficient (V/°C)		
$P_{PV}$	output power of the photovoltaic module		
$N_{PV}$	number of photovoltaic modules		
$\eta$	photovoltaic inverter efficiency		
$MTTF_j, MTTF_j$	mean time to failure and mean time to repair of the $j$ -th component		
$Up\ time_j, Down\ time_j$	duration of in-service and out-of-service state of the $j$ -th component		
$A_{segi}$	availability probability of the $i$ -th segment		
$\varepsilon$	desired accuracy level		
$E(X)$	expected value of parameter $X$		
$SOC(t, n)$	state of charge (SOC) of the $n$ -th plug-in hybrid electric vehicle (PHEV) in the $t$ -th time segment		
$\Delta LG, LUG$	difference between demand loads and generation capacities, and the largest unit of power generations		
$N_C, N_P, N, N_{SW}, N_{EMU}$	total number of cyber elements, power elements, PHEVs, switches, and EMUs		

mutual cyber-power interdependencies is interesting and essential.

The most reliability studies which considered the cyber-power interdependencies (CPIs) focused on the conceptual insights [4,8,9]. Even in references like [1,10] which developed the quantitative evaluation methods for cyber-physical system, the stochastic behaviors were not discussed, in details.

In references like [11,12], the adequacy evaluation of power systems including wind/solar DG units were studied under various uncertainties. But in such references, the eventual effects of cyber system were not concerned. On the other hand, the proposed method of [1,10] which considered the effects of cyber systems on the power networks has not been coupled to previous approaches considering the uncertainties. Hence, the authors proposed the stochastic risk management for smart grids based on direct cyber-power interdependencies (DCPIs) [13] and indirect cyber-power interdependencies (ICPIs) [14]. In [13,14], various

sensitivity analyses have been performed to investigate the pattern of DCPIs and ICPIs impacts as DG penetration level in different DG technology scenarios. Although, the stochastic-based reliability evaluation method has been in [13,14], but the uncertainty of demand-side such as PHEV charging load has been received less attention.

This paper tries to simultaneously consider the uncertainty and probabilistic behaviors of power system (supply- and demand-side) inside the DCPIs.

The introduced method is stochastic-based one using Mont Carlo simulation (MCS) [15]. But Refs. [1,10] presented the analytical approaches using P-table. Although, it is possible to develop the P-table to cover the uncertain supply and demand sides, but through using stochastic approaches similar to MCS, it would be more simplified to add the different stochastic parameters such as charging load of PHEVs as the uncertain loads. By using the MCS, it is achievable to accurate studying of stochastic behavior

of uncertain elements and systems in power systems [16], and the different stochastic parameters can be simulated over an adequately long period simulation [11]. Although through using of PHEVs the consumption of fossil fuels and gas emissions by the cars might be reduced, it will increase the electrical power demand [17]. Hence, it is essential to simulate the impacts of PHEVs charging on the adequacy and reliability of smart grid. Proposing a comprehensive method studying the important uncertainties in both power network (supply- and demand-side) and cyber network is one of the most contributions of this paper. Moreover, the well-being assessment which is a relatively new approach is performed. The studies in wide spread presence of PHEVs for modeling the eventual uncertainty of demand-side is the main contribution of this paper in compare with [13,14] as the previous works of authors. Further, the sensitivity analyses will be performed to gain insight how the increase of failures in different type of cyber elements can affect the system reliability in appropriate and inappropriate cyber topologies.

The proposed method is applied to two case studies; the first one is the practical rural distribution system introduced in [11], and the second one is a realistic 20 kV distribution system of Hormozgan regional electrical company (HREC) in Iran. The reliability indices such as expected energy not supplied (EENS), loss of load probability (LOLP), and well-being criteria are examined. The obtained results illustrate how the cyber failure adversely affects the system reliability under presence of DGs and PHEVs.

In brief, the main contributions of this paper to the field of smart grid reliability are the following:

- Development of a novel stochastic-based methodology to assess the DCPIs on the smart grid including DGs and PHEVs
- Precise simultaneously consideration of various uncertainties such as PHEV owners' behaviors, output power of renewable DG units, and DCPIs
- Introducing a general approach for studying the different types of uncertainties on the smart grid reliability by using MCS
- Well-being evaluation in addition to conventional reliability evaluation methods
- Taking into account the reliability affects due to variation of various uncertainties consist of failures in different cyber elements and power ones by sensitivity analyses
- Comparisons between the importance of different aspects of DCPIs (e.g. comparison among the impacts of energy management units (EMUs) as control elements and switches as communication ones)

This paper is organized as follows. Section 2 presents the comprehensive presentation of the proposed method. In Section 2, the proposed method based on DCPIs and modeling and simulation process of DGs and PHEVs are explained. Test case studies and test results are addressed in Sections 3 and 4, respectively. Finally, the conclusion is given in Section 5.

## 2. Comprehensive presentation of the proposed method

The first type of CPIs is the DEEI [1,2,10,13]. In this kind of CPIs, the failure occurrence on a cyber element causes a failure on the connected power one. The mal-operation or changes in the behavior of a circuit breaker that caused by a failure on the direct connected controller is an example of DEEI. This example can be found in Fig. 1 [13].

The DNEI is the second type of direct CPIs. This interdependency means that the failure in cyber network leads to the failure of corresponding element in the power network. For example, if a failure occurs in one switch of the cyber network and the data stream can-

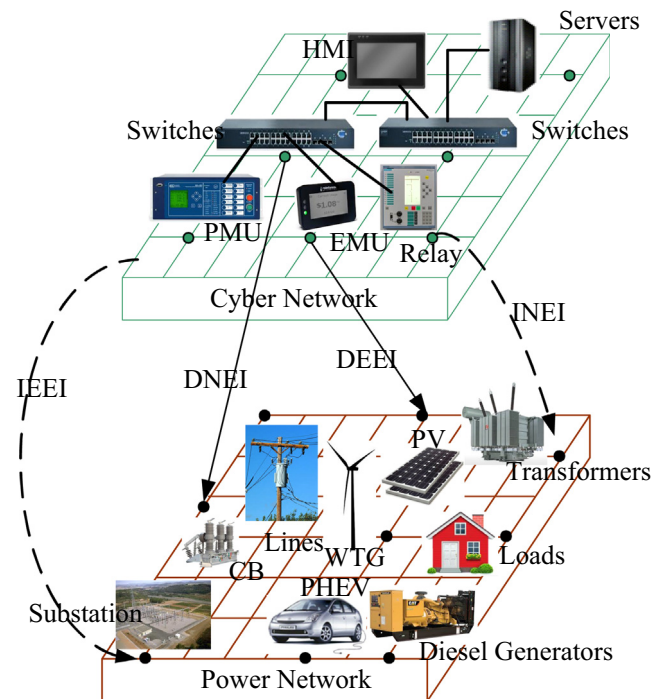


Fig. 1. A schematic showing direct and indirect CPIs of smart grid [13,14].

not flow in the other communication channel, the controller does not receive the convenient data and the power network cannot operate properly [1]. The communication failures corresponding to monitoring and protection systems are examples of INEI [10]. The failure of protective device is an example of IEEI. For instance, if a downstream protection device of distribution network such as fuse, relay, and recloser does not work properly, the performance of system does not change immediately, but the potential future failures will be intensified. The comprehensive definitions and supplementary examples regards to CPIs can be found in [13,14].

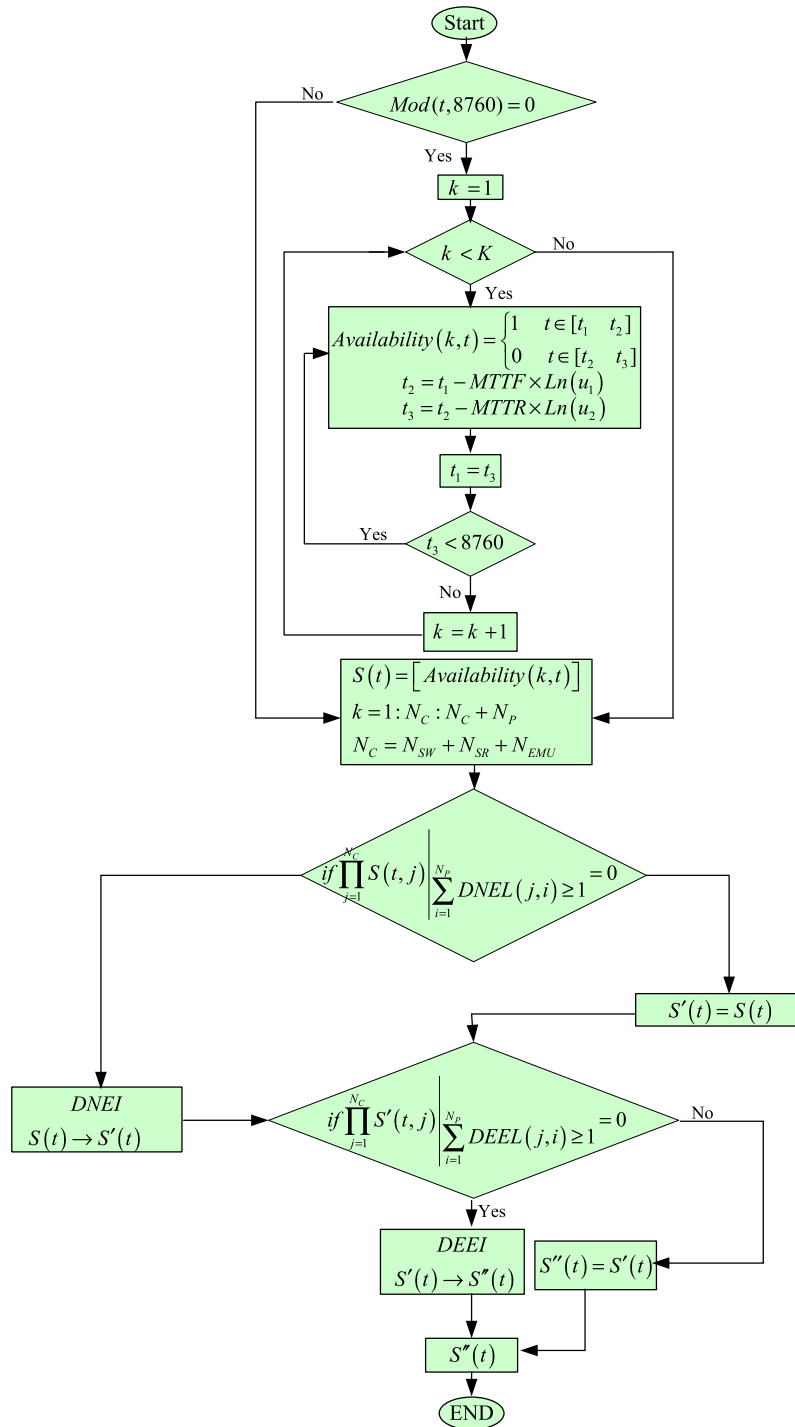
In this paper, a novel adequacy evaluation method which considers the DCPIs using MCS is proposed according to following steps:

- State initializing of smart grid in any time segment (hourly) (see flow chart shown in Fig. 2)
- State mapping and considering the direct CPIs from two heterogeneous networks into an integrated one (see flow chart shown in Fig. 2)
- Simulation of wind/solar/diesel DG units, PHEVs, and loads (see flow charts shown in Figs. 2 and 3)
- Reliability and adequacy evaluation and well-being assessment (see flow chart shown in Fig. 3)

In [13,14], the similar process except modeling of PHEVs has been proposed by the authors which focuses on the impacts of different levels of DG penetration. In this paper, the precise modeling of uncertainties regarding the demand side including the PHEVs is added. Further, the behavior of cyber elements and the sensitivity of cyber failures are mainly concerned in the sensitivity analysis to get insight into how the changes in cyber failures affect the system reliability.

### 2.1. State simulation of cyber-power system

The two-state reliability model shown in Fig. 4 is the most popular model for power systems [18–20]. To simulate the two-state



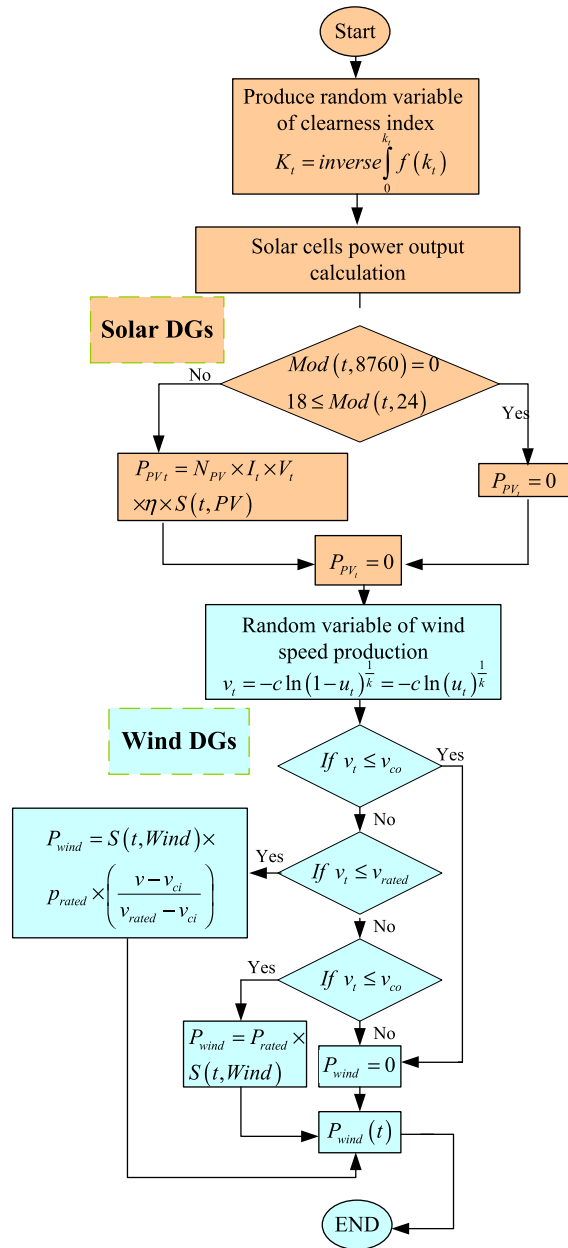
(a) State initializing and state mapping procedure

Fig. 2. Flowchart of the proposed state initializing, state mapping, and modeling of renewable DG units.

model of smart grid elements, the probability distribution of time to failure (TTF) and time to repair (TTR) must be determined. Various statistic models such as Exponential, Log-normal, Gamma, and Weibull were developed to simulate the TTF and TTR data which have the same nature as the recorded actual data. It is prevalent to use the exponential distributions for modeling the TTFs and TTRs. Most well-known reliability evaluation methods like cut-sets [21], analytical methodology [11,22,23], and the Markov process [24] were introduced based on the Exponential modeling. This

is mainly because the estimation regarding the Exponential distribution from the historical data is very simple [19].

An Exponential distribution may be appropriate for modeling of power system elements which operate in their designed useful life, but this model could not be valid for aged elements. In fact, the use of Exponential distribution to model the TTFs and TTRs is adequately accurate for elements which are not subject to “burn-in” nor are not subject to “wear”. Based on that, several studies analyzed the different distribution models for TTFs and TTRs. For



(b) Modeling of renewable DG units

Fig. 2 (continued)

instance, Zapata et al. [19] studied the model of TTR for 46 classes of electric distribution elements based on the 4-year historical data. The authors showed that the Exponential model is valid only for 50% of the studied elements, but in contrast, the Log-normal, Weibull, and Gamma distribution models are valid for 100%, 80.4%, and 69.5% of the monitored classes, respectively. Further, the literature shows that Weibull distribution is the most general used distribution for modeling of aging failure changes as a function of the operation time [25,26]. Hence, to model the TTF of an aged system, the more accurate reliability evaluation is achievable through using of Weibull distribution.

As described, it is important to get insight into how the various distribution models for TTR and TTF affect the reliability results. Nevertheless, in this paper the desired accuracy can be achieved through the use of Exponential model for up- and down-states

because the proposed reliability evaluation method focuses on the designed useful life, and the aging failures have not been concerned. It should be mentioned that for studying of the indirect CPIs as a future work of the authors, the performance of the monitoring systems and aging failures play a major role. Therefore, the more accurate simulation of up-state and TTF according to Weibull distribution and down-state according to Log-normal distribution is inevitable.

A random number generation algorithm is utilized to provide uniformly distributed samples on [0,1]. Then, the discussed samples are transformed to up- and down-state variables by using the appropriate cumulative density function (CDF). As described, in this paper, the Exponential distribution is used to simulate the two-state reliability model of system components. The up- and down-state based on the Exponential distribution can be

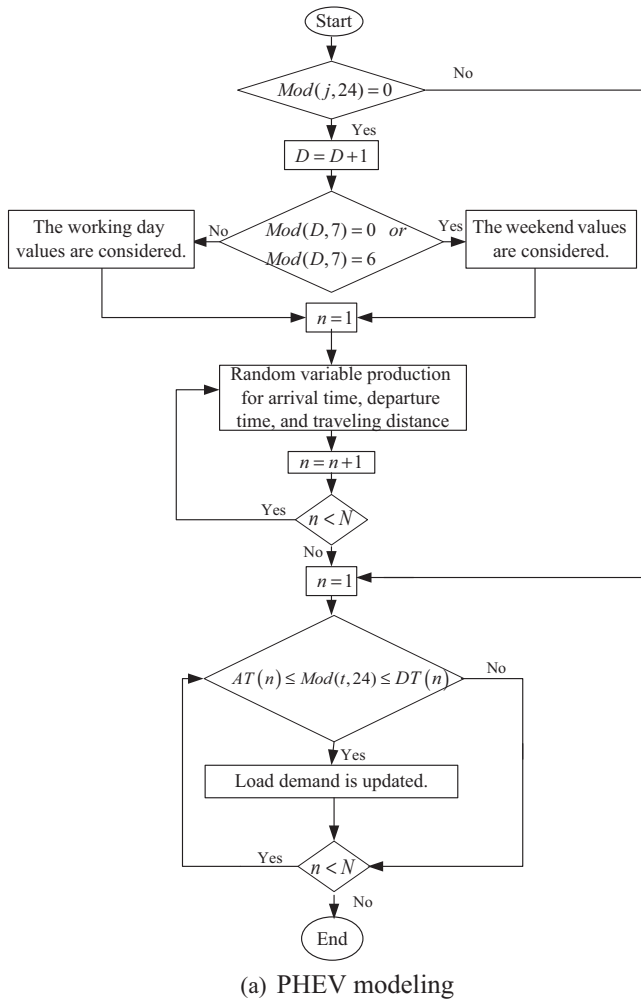


Fig. 3. Flowchart of PHEV modeling, well-being assessment, and reliability evaluation.

determined as (1) and (2) [13,27]. Then, the simulated up- and down state of different components are used to produce the system state using (3) and (4).

$$Up\ time_j = -MTTF_j \times Ln(u_1) \quad (1)$$

$$Down\ time_j = -MTTR_j \times Ln(u_2) \quad (2)$$

$$Availability(j, t) = \begin{cases} 1 & t \in Up\ time_j \\ 0 & t \in Down\ time_j \end{cases} \quad (3)$$

$$S(t) = [Availability(1, t), \dots, Availability(N_c + N_p, t)] \quad (4)$$

The value of one for  $Availability(j, t)$  means that the  $j$ -th component is in-service and the zero value represents the outage of the  $j$ -th component.

Although availability is a measure for the percentage of time which the equipment is in an operable state while reliability is a measure of how long the item performs its intended function, but the confusing between reliability and availability is usual. In fact, availability can be measured as (5), while there are two commonly used measures of reliability: mean time between failure (MTBF) and failure rate ( $\lambda$ ) as depicted in (6) and (7) [28,29]:

$$Availability = Up\ time / Total\ time\ (Up\ time + Down\ time) \quad (5)$$

$$MTBF = Total\ time\ in\ service / Number\ of\ failures \quad (6)$$

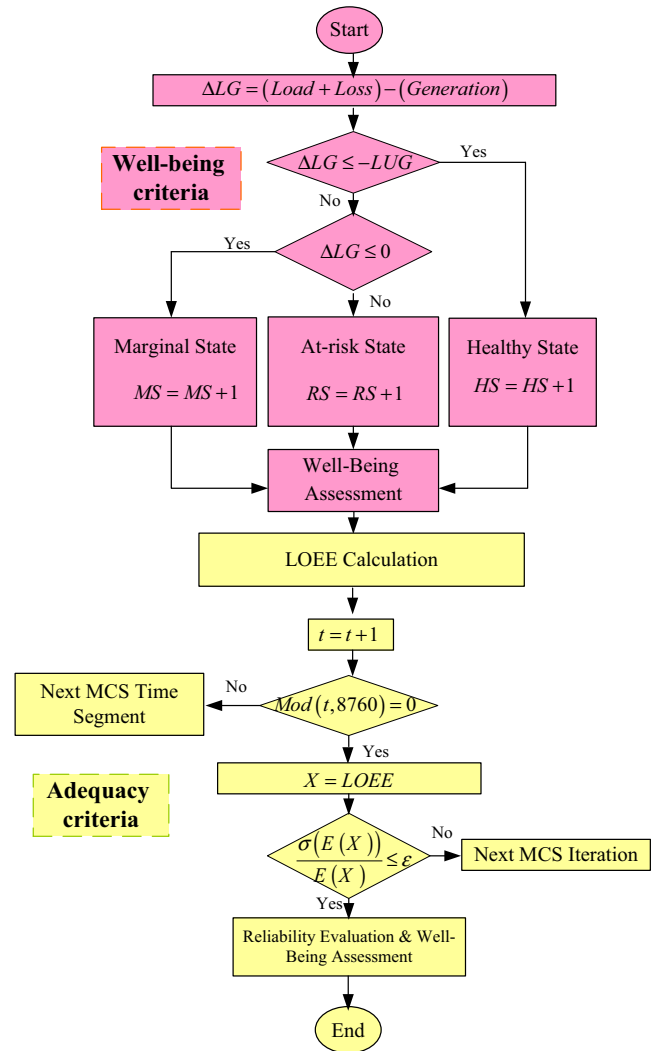


Fig. 3 (continued)

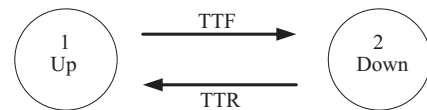


Fig. 4. Two-state reliability model of smart grid elements [13].

$$\lambda = \text{Number of failures} / \text{Total time in service} \quad (7)$$

On the contrary, the concepts of availability and reliability are twisted together. It is evident that when the availability of any system or component increases, the reliability of discussed system or element directly increases. Therefore, it is common to use these concepts instead of each other, particularly in reliability evaluation of power systems. However, the difference between availability and reliability should be carefully concerned.

The state initializing in any time segment is shown in Fig. 2. As shown, the up- and down-time series is generated at the first time segment of any MCS iteration (yearly segment), and consequently the state initializing is done. The first time segment is investigated based on the Mod function of time segment and 8760 (hours of 1-year MCS iteration). Then, for all cyber and power elements, the up- and down-states are simulated at least for 8760 h duration.



Consequently, it is possible to generate the system state for any time segment. By knowing the system state in any time segment, it is possible to judge about the CPIs and other required activities for completing the reliability evaluation. As shown in Fig. 2, the up and down times are determined by using Exponential probability model. It is necessary to generate the system state according to state of any power and cyber elements. The energy management units (EMUs), servers, and switches are considered as cyber elements which directly affect the power network. In this paper, the discussed cyber elements are studied, but it is possible to add other cyber elements with direct interdependencies to power network.

### 2.2. State mapping

In [1,2,10], an analytical state mapping methodology based on the P-table has been proposed. In this paper, the stochastic-based state mapping using MCS which was introduced in [13] is used. It should be emphasized that this stochastic-based state mapping enables us to simultaneously study various uncertainties and probabilistic variables. This is possible because of using the MCS, while it would not be easy in the analytical approaches. The discussed advantage is an important motivation to prepare the proposed state mapping approach. Accordingly, adding the modeling of PHEVs charging as one of the most important uncertainty regarding the demand side of smart grid is achievable inside the reliability evaluation based on DCPIs.

If the  $j$ -th cyber element can support its functions but does not receive the proper information from the data source, and leads to failure or mal-operation of the  $i$ -th power element, the  $DNEL(j, i)$  is set to one, otherwise the zero value is assigned to  $DNEL$  cells [13].  $DNEL$  is usually applicable during the failures of communication elements such as data cables and switches. The integration of equivalent states, particularly due to communication failures between cyber elements is also achievable.

As described in (8), if the  $j$ -th cyber element is unavailable, and there is a DNEI between the  $j$ -th cyber element and any power element, the DNEI mapping must be performed. After condition initialization for DNEI state mapping as (8), the mapping can be performed by using (9). In the target state based on DNEI mapping ( $S'$ ), if the state element of any power component has one value, it is guaranteed that it may not be affected due to DNEI. In the proposed method in [13], evaluation of all states is practically possible, although a set of states with a certain order like third order approximately covers the all states because by increasing the state order, the probability of these high order states significantly decreases.

$$\text{if } \prod_{j=1}^{N_c} S(t, j) \Big|_{\sum_{i=1}^{N_p} DNEI(j, i) \geq 1} = 0 \Rightarrow \text{DNEI Mapping : } S(t) \rightarrow S'(t) \quad (8)$$

$$S'(t, i) = \begin{cases} S(t, i) & \text{else.} \\ S(t, i) \times S(t, j) & \text{if } DNEI(j, i) = 1 \end{cases} \quad (9)$$

Similar to  $DNEL$ , creating the  $DEEL$  matrix is the first step of  $DEEL$  mapping procedure [13]. As it can be seen in (10), if the product of state elements regarding the elements having a  $DEEL$  is equal to zero, the state mapping starts. The zero value of the product of discussed cyber elements means that any failure of any cyber element is enough to start the  $DEEL$  mapping. Further to determine that the  $j$ -th cyber element has a  $DEEL$ , the sum of the respective  $DEEL$  ( $\sum_{i=1}^{N_p} DEEL(j, i)$ ) must be determined, and it's greater than or equal to one value implies that there is a  $DEEL$ . Then, the system state is updated as (11), and the elements of state

vector corresponding to the power element which is interconnected to specified cyber elements are multiplied to state elements belongs to the discussed cyber elements.

$$\text{if } \prod_{j=1}^{N_c} S'(t, j) \Big|_{\sum_{i=1}^{N_p} DEEL(j, i) \geq 1} = 0 \Rightarrow \text{DEEL Mapping : } S'(t) \rightarrow S''(t) \quad (10)$$

$$S''(t, i) = \begin{cases} S'(t, i) & \text{else.} \\ S'(t, i) \times S'(t, j) & \text{if } DEEL(j, i) = 1 \end{cases} \quad (11)$$

As shown in Fig. 2, firstly if any failure occurs in any cyber element, the  $DNEI$  mapping is started. Secondly, the  $DEEL$  shall be followed. The  $DNEI$  state mapping starts if (8) is happened, otherwise, the  $DNEI$  mapped state ( $S'(t)$ ) remains as ( $S(t)$ ) without any changes. Afterwards, the same procedure is repeated based on (10). If it is necessary to  $DEEL$  mapping, the  $S'(t)$  is mapped to  $S''(t)$ .

By investigation of  $S''(t)$  including  $DNEI$  and  $DEEL$  mapping, it is possible to evaluate the system reliability as a conventional power system without any CPIs.

### 2.3. Wind speed modeling and calculation of the output power of wind DG units

The wind speed is simulated based on (13) [30–34]. Afterwards, the output power of wind-based DG units is calculated as shown in (14) and Fig. 2 [33–36] as a function of simulated wind speed.

$$V = -c \ln(1 - u)^{\frac{1}{k}} = -c \ln(u)^{\frac{1}{k}} \quad (12)$$

$$P_W(v) = \begin{cases} 0 & 0 < v < v_{ci} \text{ OR } v_{ct} > v \\ P_{rated} \times \frac{(v - v_{ci})}{(v_r - v_{ci})} & v_{ci} < v < v_r \\ P_{rated} & v_r < v < v_{ct} \end{cases} \quad (13)$$

The detailed explanations about the simulation of output power for wind turbine DG units can be found in [13,14].

In Fig. 2(b), the modeling of the wind-based DG units is shown. In the presented flowchart, it is obvious when the wind speed is out of range (higher than cut-off speed or less than cut-in speed), the output power of the DG unit is zero. In addition, for wind speed values in range of rated and cut-off speed for wind turbine, the rated output power is achievable. Otherwise, the output power is calculated according to (14) as a proportion of the rated power.

### 2.4. Solar irradiance modeling and calculation of the output power of solar-based DG units

The output power of solar-based DG units is calculated for a specified solar irradiance, ambient temperature, etc. as (15)–(18) [37–39]. The more detailed explanations about the modeling of solar-based DG units have been given in [13,14] by the authors.

$$k_t = \frac{G}{G_0} \quad (14)$$

$$T_c = T_a + \left( G \times \frac{(N_{OT} - 20)}{800} \right) \quad (15)$$

$$I = k_t \times (I_{sc} + (T_c - T_a) \times K_I) \quad (16)$$

$$V = V_{oc} - k_V \times T_c \quad (17)$$

$$P_{PV} = N_{PV} \times I \times V \times \eta \quad (18)$$

The above modeling and corresponding equations for solar-based DG units can be found in Fig. 2(b). As shown in this flowchart, the random number generation is necessary to determine

the solar clearness index. Then, the output power is calculated based on the above equations when the sun shines and the solar irradiance is considerable.

### 2.5. PHEV modeling and calculation of the uncertain loading of PHEVs charging

The PHEVs owners' behaviors such as the departure time, arrival time, and the traveling distance have uncertain nature [40–42]. It is important to determine the appropriate probability distribution of arrival time, departure time, and the traveling distance of electrical vehicles. Also, the charging schedule is another important characteristic of PHEVs. The state of charge (SOC) for PHEVs in any time segment of MCS is investigated to evaluate its charging demand load as (19). Thus, the load data is upgraded similar to flowchart shown [40]. In Fig. 3(a), the flowchart for modeling the PHEVs is shown. As shown in this figure, firstly it is determined that the simulated day is weekend or working day. The determination of working days and non-working days is necessary because the drivers' behaviors are different in working days and weekends. According to this classification, the values of probability distribution models for departure time, arrival time, and traveling distance are assigned to the understudy PHEVs.

To model the arrival time, departure time, and the driving distance of PHEVs, the simulated variables based on the inverse of appropriate CDFs must be generated. The normal distribution can be used for statistic modeling of arrival time and the driving distance of PHEVs. The probability function of departure time of PHEVs in workdays is usually different from arrival time because the most vehicle owners leave the home about a certain time like 7:00 AM. Therefore, the simulated variable corresponding to the departure time of PHEV is generated according to Weibull distribution [40].

$$SOC(t+1, n) = \begin{cases} SOC(t, n) - R_{cons}^n \Delta x(t, n) & \text{Driving} \\ SOC(t, n) + R_{chg}^n \Delta t(t, n) & \text{Charging} \\ SOC(t, n) & \text{else.} \end{cases} \quad (19)$$

As it can be seen in Fig. 3 and above explanations, determining the PHEV owners' behaviors is a function of workdays and weekends. Next according to be in workday or weekend, by using a random number generation and inverse of appropriate CDFs, the simulated variables are provided.

As it shown in Fig. 3(a), the demand load update is performed if the simulated time is in range of arrival time and departure time. In fact, when the PHEV is not connected to grid, no load update due to PHEV charging is needed. The PHEV can be charged through the grid since arrival time up to departure time. In this time, it is necessary to calculate the upgraded demand load which considers the PHEV charging load. Further, in order to reduce the calculations and computing time, the load updating process can be stopped when the PHEV has been fully charged. This process is done for all PHEVs. Afterwards, the charging demand load is investigated

and accordingly the aggregated load consists of conventional loads and PHEVs' charging demand load is calculated.

The authors proposed a precise method for modeling the PHEVs charging in different charging schedules in [42]. In [42], the unmanaged charging, managed charging, and vehicle to grid (V2G) have been studied. In this paper, the authors tried to combine the PHEV modeling to DCPI-based reliability evaluation method. The modeling of PHEVs is added in order to simulate the uncertainty of demand side through system reliability evaluation beside the DCPIs. Until now, there is no study which integrated the study of DCPIs and PHEVs. This paper tries to response this matter.

### 2.6. Modeling of load and diesel generators

The diesel generators are assumed to be dispatchable DG units [43]. Also, the load profile of conventional customers without charging demand load of PHEVs is assumed that following the IEEE-RTS system [44]. Since the variations of conventional loads is less than the other probabilistic parameters such as solar irradiance and wind speed, it is possible to assume that the load is invariant during the simulation time segment. However, through updating the load value by adding the PHEV charging demand load as an uncertain load, the appropriate modeling of the demand side was carried out.

### 2.7. Well-Being assessment

In well-being assessment, there are three states based on the power balance condition [13,42,45]: healthy, marginal, and at-risk states. Fig. 5 shows the well-being model. Also as shown, the at-risk state can be categorized into emergency and extreme emergency states [45].

$$P_{G,DGs}(t) + P_{MainSub}(t) \geq P_{Loads}(t) + P_{PHEVChg}(t) + P_{Loss}(t) \quad (20)$$

$$C_R(t) \geq C_{LU}(t) \quad (21)$$

In addition to meet the (20) and (21), the power flow equations, voltage limits, and transmission limits as the major constraints should be satisfied [46,47]. These conditions and constraints are shown as presented in (22)–(24)

$$P_{MainSub} + \sum P_{DGs} - \sum P_{Load} = \sum_{i=1}^{nbus} V_{t,i} \times V_{t,j} \times Y_{ij} \times \cos(\theta_{ij} + \delta_{t,j} - \delta_{t,i}) \quad \forall i, t \quad (22)$$

$$\begin{aligned} V_{min} &\leq V_{t,i} \leq V_{max} \quad \forall i \neq 1 \\ V_{t,1} &= 1.05 \end{aligned} \quad (23)$$

$$P_l \leq P_{max,l} \quad \forall l. \quad (24)$$

Furthermore, the necessary condition for successful operation of grid in islanding mode is as (25) [48]. As it can be seen, the penetration level of dispatchable DG units should meet the islanding success index. It means that at least a certain percentage (for instance 60% [48]) of the total DG generation in the island should be dispatchable.

$$P_{DDG} \geq K_{D2T} \times P_{G,DGs} \quad (25)$$

In Fig. 3(b), the well-being assessment is shown. In any MCS time segment, the difference between power generation and losses and loads is calculated. According to this difference, it is possible to determine the available reserve or power shortage. Then, the system state (healthy, marginal or at-risk state) is evaluated.

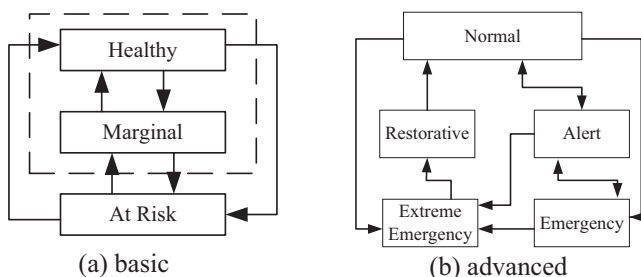
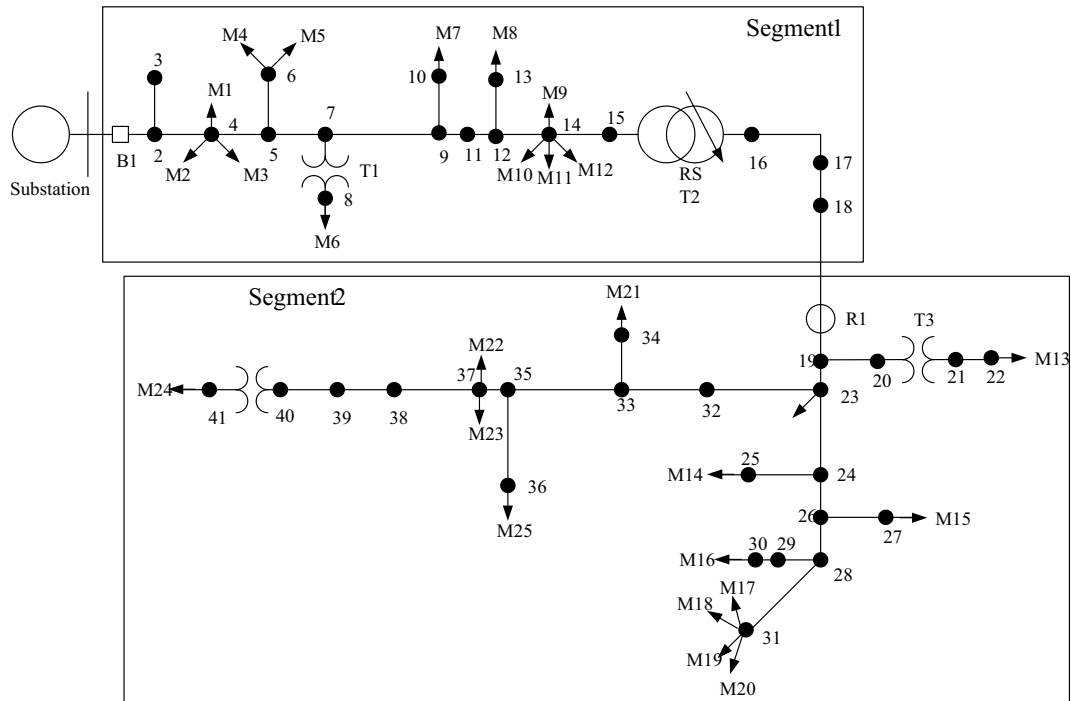
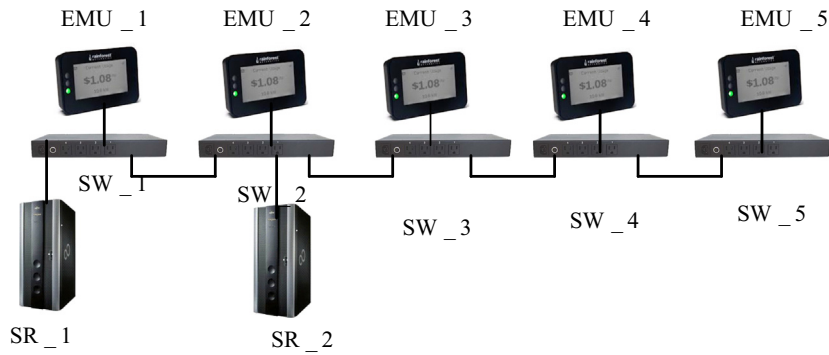


Fig. 5. System well-being model.





(a) Single line diagram of the power network



(b) Cyber network topology

Fig. 6. The first case study similar to that presented in [11,23].

Table 1

Direct element-element CP-links between control and power elements for the first case study.

Control element	Power element
EMU_1	Substation
EMU_2	Substation
EMU_3	DG_1 (bus 28), Segment 1
EMU_4	DG_2 (bus 39), Segment 2
EMU_5	DG_3 (bus 39), Segment 2

### 3. Case studies

The proposed method is applied to two practical distribution systems; the first one is the practical rural distribution system introduced in [11,23], and the second one is an actual 20 kV distribution system of Hormozgan regional electric company (HREC) in Iran which has been considered as a pilot system for upgrading to smart distribution grid [13,14,42].

#### 3.1. First case study

The single line diagram of the first case study is shown in Fig. 6. The test system information is given in [11]. This test system consists of three types of DG units (diesel, wind-based, and PV-based DG units). The DG units are connected to buses 28 and 39. The assumed cyber network of this test system has been shown in Fig. 6(b). In addition, the CPIs have been listed in Table 1. This test system is chosen in order to simplify the justification about the

#### 2.8. Reliability and adequacy evaluation

As presented in Fig. 3, firstly the supply- and demand-side parameters are investigated, and then the adequacy evaluation is performed based on eventual power shortage [49]. By using the MCS, the stochastic-based simulation is done, and the discussed process continues in order to obtain the desired accuracy.

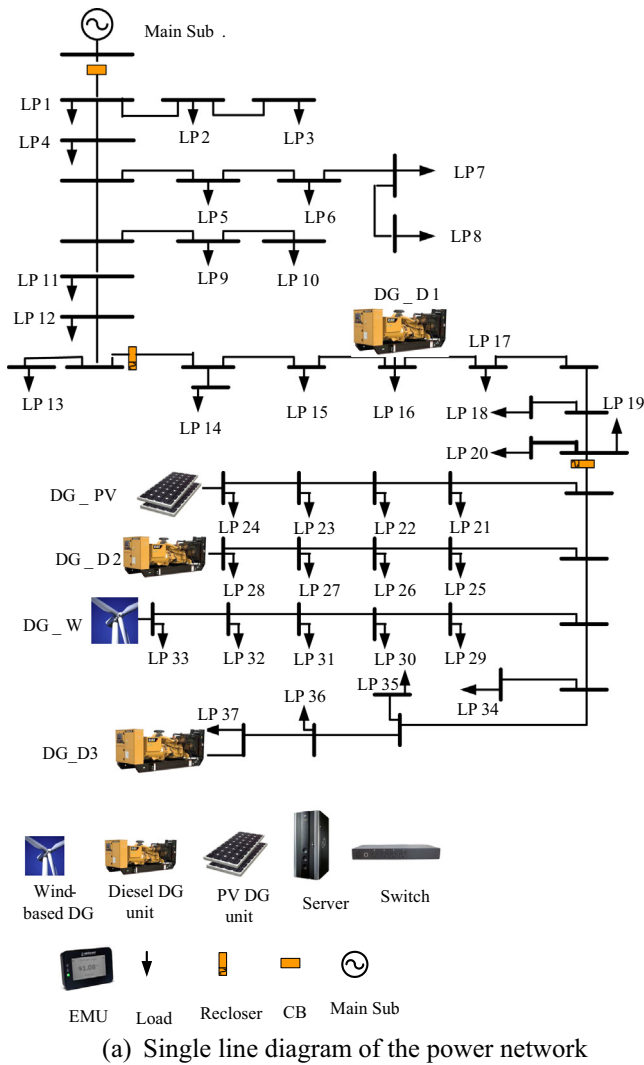


Fig. 7. Second test system [13].

contributions of the proposed methodology. Further, the comparison results between the results highlight the advantages of this article. The comparison results (ones based on [11,23] and ones based on the proposed method) emphasize the importance of using the proposed method because the inaccuracy in reliability results due to neglecting the DCPIs is inevitable.

3.2. Second case study

The power network of the second case study is shown in Fig. 7. In this figure, the appropriate and inappropriate cyber networks are shown. The main substation supplies the system from the bulk power system has been equipped with four 1.5 MW transformers. As shown, three protective devices are located in the sending bus of sections 1, 17 and 27, respectively. Therefore, the system is divided into three segments with aggregated peak loads of 1.847, 1.300, and 2.940 MW without PHEV charging load demands, respectively.

Five DGs have been connected to the grid. The first type of DG units is diesel DG consists of one and two diesel generators each of 900 kW connected to load points 16 in the second segment and load points 28 and 37 of the third segment. The second type of DGs is solar-based DG unit of 375 kW connected to load point 24 in the second segment, and the third one is wind-based DG unit of 375 kW connected to load pint 33 in the third segment.

As shown in Fig. 7, the cyber system (which consists of 7 EMUs) controls the output power of DG units and the main substation. The main substation condition is more concerned, therefore the cyber network configuration supports it using two EMUs connected to different switches. The main substation is just influenced by cyber failures, if a double contingency simultaneously occurs in the EMUs 1 and 7 or in switches 6 and 7. The direct element-element CP-links between control and power elements for the second case study are listed in Table 2. The cut-in, rated, and cut-off values of the wind-based DG unit are 4, 14, and 25 m/s. Moreover, the characteristics of PV modules can be found in [50].

The MTTF and MTTR of power elements (e.g. wind-based DG units, PV modules, diesel DG units, and transformers) and cyber ones (e.g. switches, EMUs, and servers) are driven from data of

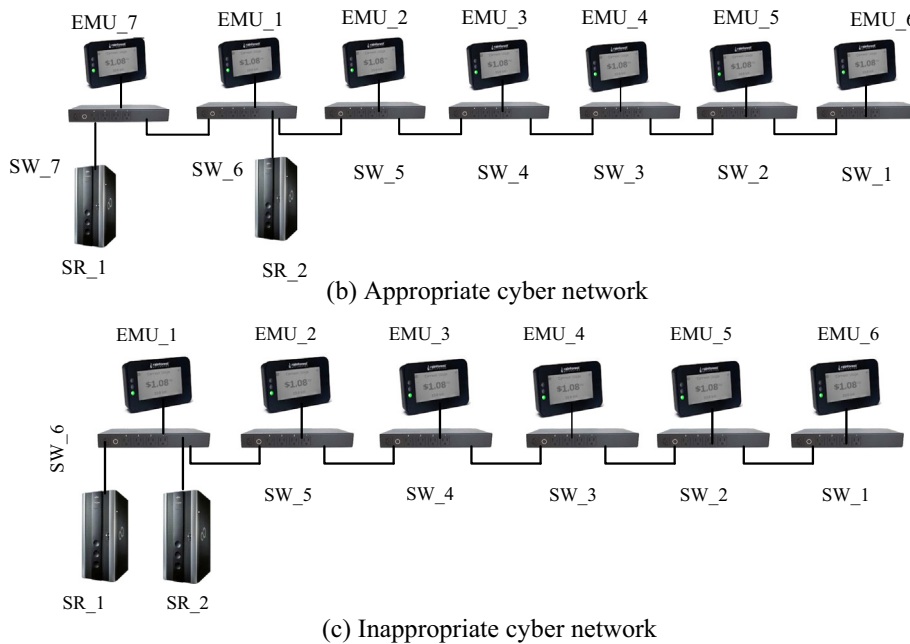


Fig. 7 (continued)

[1,51]. The failure rates of segments have been considered to be 0.2057%, 0.5870%, and 0.13883% failure/year according to historical data.

The system operates in connected mode if at least one transformer of the main substation is in-service and the circuit breaker connecting the bulk power system to the distribution system is closed. If two discussed conditions were not satisfied, the smart grid works in islanding mode. In addition to fully connected or islanding modes, it is possible that the segment 1 operates in connected mode while a failure in segment 2 leads to disconnect the other segments from the bulk power system. In this condition, the loads of segment 3 can be supplied in islanding mode.

The peak load of PHEV charging is approximated to be 370, 260, and 588 kW in the segment 1, 2, and 3, respectively. When the 124, 87, and 196 PHEVs are charged through the 20/0.4 kV transformers, the load growth will be about 20%. The home-charging is just feasible and the charging level is assumed to be about 3 kW. The mean value of PHEVs electric energy consumption and energy storage system capacity are considered 0.4 kWh/km and 25 kWh, respectively [52].

#### 4. Test results

##### 4.1. Results of first case study

The adequacy and well-being results of the first case study based on ideal cyber systems and actual ones are presented in Table 3. In addition, the results based on the proposed method and those obtained by [11] have been compared together. The obtained results for ideal cyber networks according to the proposed method are compared to the analytical- and MCS-based results of [11]. This comparison analyses confirm the validation of the proposed method. The comparison results between ideal cyber network (similar to what introduced in [11]) and those of actual cyber and power networks imply that the system reliability is significantly affected due to direct CPIs. The loss of load expected (LOLE) and LOEE have been increased by more than 20% due to direct CPIs, and the healthy period has been reduced. It infers that the reliability evaluation of smart grid without consideration of CPIs cannot be adequately accurate. Accordingly, the importance of considering of the CPIs is emphasized. Therefore, the proposed method will be interesting in order to reliability evaluation of smart grids.

**Table 2**  
Direct element-element CP-links between control and power elements for the second case study.

Control element	Power element
EMU_1	Main Sub.
EMU_7	Main Sub.
EMU_2	DG_D1 (LP16), Segment 2
EMU_3	DG_PV (LP24), Segment 3
EMU_4	DG_D2 (LP28), Segment 3
EMU_5	DG_W (LP33), Segment 3
EMU_6	DG_D3 (LP37), Segment 3

**Table 3**  
Adequacy and well-being results of the first case study under various scenarios.

Adequacy indices and well-being criteria	Scenario 2: Cyber network is ideal (failure free)		Scenario 4: Cyber network is not ideal	
	Results presented in [11]		Proposed method	
	Analytical	MCS		
LOLE (h/year)	10.4281	9.4546	10.3636	12.4839
LOEE (MWh/year)	25.5544	24.4351	25.3612	33.5426
Healthy period (hr/year)	8537.3814	8530.87	8532.2417	8414.7082
Marginal period (hr/year)	229.772	223.462	217.3947	332.8079

##### 4.2. Results of second case study

The results such as LOLP, EENS, and well-being criteria of second case study under various scenarios are discussed. The test results illustrate how the CPIs can adversely affect the system adequacy. Also to clarify the importance of cyber network configuration, the test system using an infirm cyber network configuration shown in Fig. 7 is also studied.

The at-risk period due to the CPIs is increased by about 27% (from 8.69 h without CPIs to 11.052 h by considering the CPIs). The cyber network failures lead to 28.72 h reduction of healthy period. It is obvious that the inappropriate cyber network configuration highlights the impacts of CPIs. Through using an inappropriate cyber network configuration, the period of at-risk state has been significantly increased. The 50.96 h of at-risk period is very greater than 11.052 h of those corresponding to the system uses an appropriate cyber network configuration.

In Fig. 8, the second case study is simulated under following scenarios:

- Scenario 1: Power and cyber networks are ideal.
- Scenario 2: Cyber network is ideal (failure free).
- Scenario 3: Power network is ideal (failure free).
- Scenario 4: Both cyber and power networks are not failure free.

The discussed scenarios are examined for appropriate and inappropriate cyber networks as shown in Fig. 7.

Scenario 1 is concerned for highlighting the adequacy evaluations and checking the power balance condition during any eventual power shortage. But, Scenario 2 is used for simulating the smart grid based on the available approaches. In this scenario, similar to conventional methodologies, the DCPIs are neglected. The results (comparison between results for scenario 1 and scenario 2) inferred that the power failures in normal conditions based on the power system topology, system aging failures, etc. does significantly increase the EENS and LOEE (loss of expected energy). It should be noted that this conclusion is not general for any system. In fact, if the system topology is not satisfied or the failures in power elements due to aging have been increased, the increase in EENS and LOEE can be considerable. As expected, in scenarios 1 and 2, the results of the appropriate and inappropriate cyber network topology are similar together.

By comparing the results under scenarios 2 and 4, it is possible to judge how the DCPIs affect the system reliability. In scenario 2, the system reliability is evaluated based on the available approaches. In the other words, the difference between EENS or LOEE in scenario 4 and scenario 2 has been occurred due to neglecting the DCPIs.

In Fig. 8, the LOEE is concerned for states where the capacity of power supply is insufficient. In addition, the EENS is considered for studying all the at-risk states caused by both insufficient power supply capacity and disconnecting the faulty area.

According to the test results shown in Fig. 8, the inaccuracy in LOEE due to CPIs is more considerable than EENS. Therefore, the

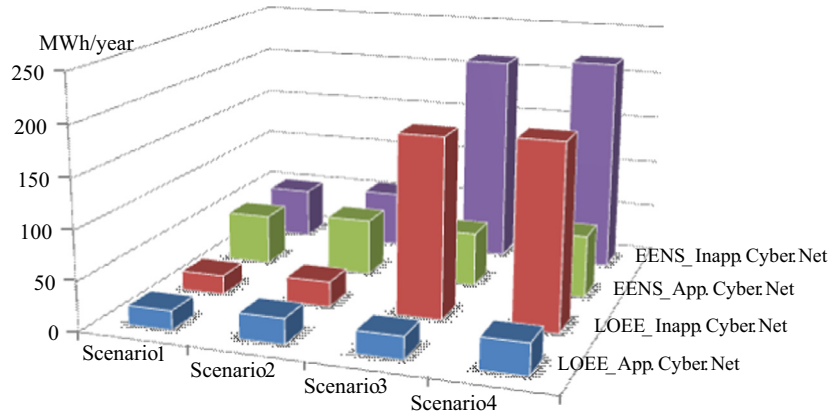


Fig. 8. LOEE due to insufficient capacity of power supply and EENS under various scenarios.

Table 4 Well-being criteria results.

Well-being states	Ideal cyber net	Appropriate cyber net	Inappropriate cyber net
Healthy period (h/year)	8725.42	8696.7	8668.28
Marginal period (h/year)	25.89	52.25	40.76
At risk period (h/year)	8.69	11.05	50.96

more detailed discussion about LOEE in different scenarios can be more useful.

The comparison results between scenario 2 and 4 for appropriate cyber network topology show that inaccuracy in LOEE or EENS due to neglecting the DCPIs is about 20%. But, the similar comparison analyses for inappropriate cyber network topology depict that the LOEE of scenario 4 is more than 3 times of those corresponding to the scenario 2. Accordingly, it is concluded that the DCPI impacts is extremely highlighted if the cyber system topology is inappropriate. This fact emphasizes the importance of using the proposed method in order to accurate reliability evaluation of smart grids.

The difference among EENS of appropriate cyber network and that of inappropriate cyber network in scenario 4 illustrates that the optimization of cyber network topology and determining a good solution is essential subject.

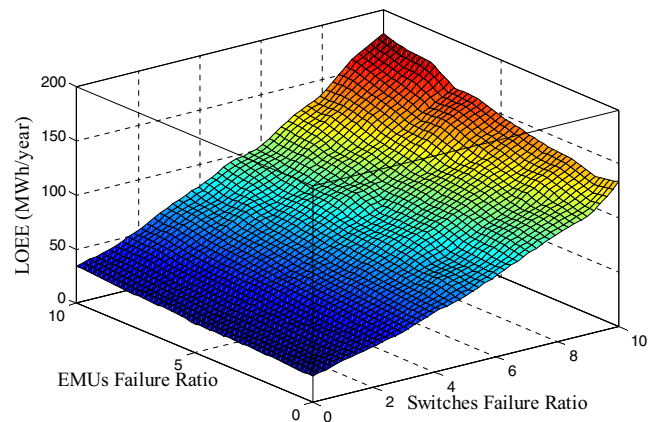
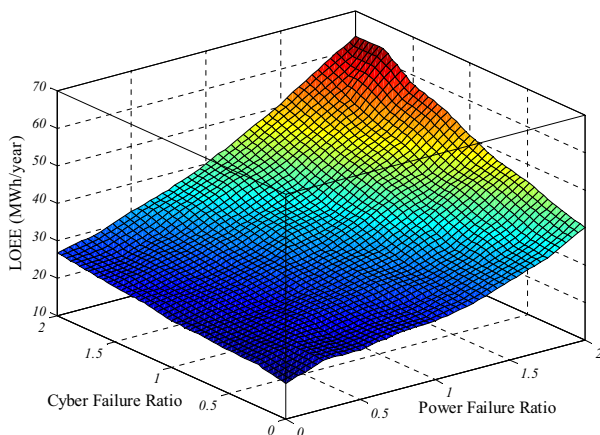


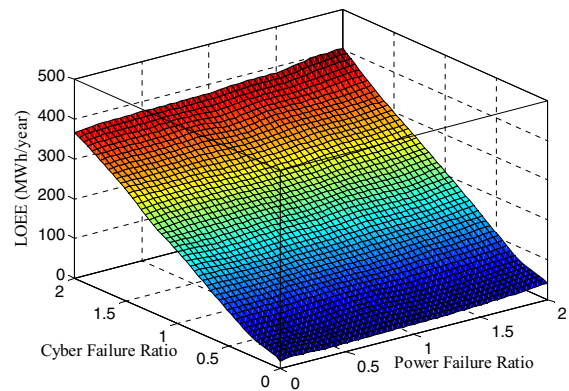
Fig. 10. Sensitivity analysis of switches and EMUs failures on LOEE.

Briefly, the values of reliability indices not considering the CPIs may not be accurate, and according to the satisfactory of cyber network configuration, the tolerances can be seriously increased.

For highlighting the importance of cyber and power failures, it is necessary to simultaneously study of scenarios 2, 3, and 4. It is concluded that the power failures are more important than cyber failure if the cyber network has an appropriate topology. But, the



(a) Under appropriate cyber network



(b) Under inappropriate cyber network

Fig. 9. Sensitivity analysis of power and cyber failures on LOEE.



**Table 5**  
LOEE of different scenarios of EMUs and switches adjusting coefficients.

Scenario	Switch failure ratio	EMU failure ratio	LOEE (MWh/year)
A	0	0	24.31
B	0	1	25.03
C	1	0	31.76
D	1	1	34.20
E	0	10	34.63
F	10	0	133.54
G	10	10	178.42

cyber failures should be more concerned than power failures in reliability evaluation if the cyber network is not reliable. This conclusion is examined again by sensitivity analyses in the following (see Table 4).

Further, to highlight the effects of the probability distribution used for modeling the TTR and TTF (up- and down-state), the Weibull and Log-normal distributions are examined. The EENS under scenario 2 implies that about 1.36% increasing has appeared from 25.641 MWh/year (for Exponential probability distribution function) to 25.989 MWh/year (for Log-normal distribution function). It can be concluded that the inaccuracy in results due to use of Exponential distribution model and its simplifications is reasonable and negligible. However, this conclusion is not generic and cannot be applied to any distribution system, particularly for aged distribution systems.

To evaluate the reliability indices due to change of power and cyber failures, the sensitivity analysis on LOEE has been performed as shown in Fig. 9. In these figures, the LOEE value under various power and cyber failures is calculated. It seems that the LOEE is more affected due to CPIs in compare to power failures. Based on that, it seems that the CPIs will be more important if the cyber network configuration is not robust against the failure of any cyber element.

It is useful to evaluate the priority of cyber elements based on their effects on the system adequacy. Hence, the sensitivity analysis according to adjusting coefficients regarding the switches and EMUs has been done. The EMUs and switches are important elements of cyber networks, but based on their tasks and duties, their effects on CPIs can be different. The sensitivity analysis results of EMUs and switches failure adjusting coefficient between [010] are shown as Fig. 10. As it can be seen, the increase in LOEE and other adequacy indices due to adjusting coefficients of switches is more considerable than of EMUs.

The results of Table 5 imply that the adequacy evaluation without considering the switch failures is less accurate than the scenario which assumes EMUs are failure free. The LOEE increasing due to increasing of switches and EMUs' failures with adjusting coefficient from 0 (scenario A) to 10 (scenario E and F) are about 450% and 42%, respectively. This is mainly because any EMU failure leads to forced outage of one power generation source. But during any switch failure, the desired performance of more than one power element is interrupted. If the switch is located in near of the servers and there are some cyber elements in its downstream, the discussed switch is a critical point and consequently the corresponding CPIs will be more emphasized.

## 5. Conclusion

In this paper, a new reliability evaluation method simultaneously considering the DCPIs, DGs, and PHEVs in smart grid has been proposed. The proposed method comprehensively studies either the uncertainties of power systems (supply side and demand side). The stochastic output generation of renewable resources, the behaviors of PHEV owners, availability of physical elements, etc. or

cyber elements (like failures in EMUs, switches, and servers) are concerned as power and cyber uncertainties. Another advantage of the proposed method is ability to examine the well-being criteria such as healthy, marginal, and at-risk probabilities in addition to conventional adequacy indices like LOEE, EENS, and LOLP.

The various sensitivity analyses have been performed to take into account the impacts of cyber and power failure variations for appropriate and inappropriate cyber network configurations. The sensitivity analyses show that the cyber network configuration can increase the CPIs impacts. As revealed by the test results, using the conventional reliability evaluation methods not considering the cyber failures cannot be adequately accurate. This fact is highlighted in systems which utilize an inappropriate cyber network configuration. Moreover, it is inferred that the system reliability can be more affected due to communication failures in compare to controlling elements causing DEEI like EMUs. In addition, the comprehensively reliability evaluation based on DCPIs in widespread presence of PHEVs is another contribution of this paper.

## References

- [1] Falahati B, Yong F, Lei W. Reliability assessment of smart grid considering direct cyber-power interdependencies. *IEEE Trans Smart Grid* 2012;3(3):1515–24.
- [2] Falahati B, Fu Y. A study on interdependencies of cyber-power networks in smart grid applications. Presented at the IEEE ISGT, Washington, DC; 2012.
- [3] Stefanov A, Liu CC, Govindarasu M, Wu SS. SCADA modeling for performance and vulnerability assessment of integrated cyber-physical systems. *Int Trans Electr Energy Syst* 2013; PP(99): 1–22. <http://dx.doi.org/10.1002/etep.1862>.
- [4] Singh C, Sprintson A. Reliability assurance of cyber-physical power systems. In: Power and energy society general meeting, 2010 IEEE; 25–29 July 2010. p. 1–6.
- [5] Zhang L, Li K, Li K, Xu Y. Joint optimization of energy efficiency and system reliability for precedence constrained tasks in heterogeneous systems. *Int J Electr Power Energy Syst* 2016;78(1):499–512.
- [6] Zhang L, Li K, Xu Y, Mei J, Zhang F, Li K. Maximizing reliability with energy conservation for parallel task scheduling in a heterogeneous cluster. *Inf Sci* 2015;319(1):113–31.
- [7] Li K, Tang X, Veeravalli B, Li K. Scheduling precedence constrained stochastic tasks on heterogeneous cluster systems. *IEEE Trans Comput* 2015;64(1):191–204.
- [8] Kirschen D, Bouffard F. Keep the lights on and the information flowing, a new framework for analyzing power system security. *IEEE Power Energy Mag* 2009; 50–60.
- [9] Chee-Wooi T, Chen-Ching L, Govindarasu M. Anomaly extraction and correlations for power infrastructure cyber systems. In: Systems, man and cybernetics, 2008. SMC 2008. IEEE international conference on; 12–15 Oct. 2008. p. 7–12.
- [10] Falahati B, Fu Y. Reliability assessment of smart grid considering indirect cyber-power interdependencies. *IEEE Trans Smart Grid* 2014;5(4):1677–85.
- [11] Atwa YM, El-Saadany EF, Salama MMA, Seethapathy R, Assam M, Conti S. Adequacy evaluation of distribution system including wind/solar DG during different modes of operation. *IEEE Trans Power Syst* 2011;26(4):1945–52.
- [12] Liu B, Zhang Y, Liu C, He W, Bao H. Reliability evaluation for distribution systems with distribution generation. *Euro Trans Electr Power* 2010;20(7):915–26.
- [13] Hashemi-Dezaki H, Askarian-Abyaneh H, Haeri-Khiavi H. Impacts of direct cyber-power interdependencies on smart grid reliability under various penetration levels of microturbine/wind/solar distributed generations. *IET Gener Transm Distrib* 2016;10(4):928–37.
- [14] Hashemi-Dezaki H, Agah SMM, Askarian-Abyaneh H, Haeri-Khiavi H. Sensitivity analysis of smart grids reliability due to indirect cyber-power interdependencies under various DG technologies, DG penetrations, and operation times. *Energy Convers Manage* 2016;108:377–91.
- [15] Surender Reddya S, Bijweb PR, Abhyankar AR. Optimum day-ahead clearing of energy and reserve markets with wind power generation using anticipated real-time adjustment costs. *Int J Electr Power Energy Syst* 2015;71(1):242–53.
- [16] Hosseini SA, Vahidi B, Askarian-Abyaneh H. A seven-state Markov model for determining the optimal operating mode of distributed generators. *J Renew Sustain Energy* 2015; 7(5). <http://dx.doi.org/10.1063/1.4921658>.
- [17] Arifa AI, Babar M, Imthias Ahamed TP, Al-Ammara EA, Nguyen PH, René Kamphuis IG, Malika NH. Online scheduling of plug-in vehicles in dynamic pricing schemes. *Sustain Energy, Grids Networks* 2016; 7(1): 25–36.
- [18] Murthy C, Roy DS, Mohanta DK. Reliability evaluation of phasor measurement unit: a system of systems approach. *Electr Power Compon Syst* 2015;43(4):437–48.
- [19] Zapata CJ, Silva SC, Burbano OL. Repair models of power distribution components. In: Transmission and distribution conference and exposition: latin America, 2008 IEEE/PES; 13–15 Aug. 2008. p. 1–6.



- [20] Sabouhi H, Abbaspour A, Fotuhi-Firuzabad M, Dehghanian P. Reliability modeling and availability analysis of combined cycle power plants. *Int J Electr Power Energy Syst* 2016;79(1):108–19.
- [21] IEEE recommended practice for the design of reliable industrial and commercial power systems – Redline. IEEE Std. 493–2007 (Revision of IEEE Std 493–1997) – Redline; June 25 2007. p. 1–426.
- [22] Kjolte G, Sand K. RELRAD – an analytical approach for distribution system reliability assessment. *IEEE Trans Power Deliv* 1992;7(2):809–14.
- [23] Atwa YM, El-Saadany EF, Guise A-C. Supply adequacy assessment of distribution system including wind-based DG during different modes of operation. *IEEE Trans Power Syst* 2010;25(1):78–86.
- [24] Billinton R, Allan RN. Reliability evaluation of engineering systems: concepts and techniques. Plenum Press; 1992.
- [25] Zhang X, Gockenbach E, Wasserberg V, Borsi H. Estimation of the lifetime of the electrical components in distribution networks. *IEEE Trans Power Deliv* 2007;22(1):515–22.
- [26] Agah SMM, Hashemi H, Azad E, Nafisi H, Safaie A. Effect of distributed generations on aging failure probability of distribution transformers. *Electr Power Compon Syst* 2012;40(13):1470–85.
- [27] Aghaebrahimi MR, Mehdizadeh M. A new procedure in reliability assessment of wind-diesel islanded grids. *Electr Power Compon Syst* 2011;39(14):1563–76.
- [28] Chouairi A, El Ghorbal M, Benali A. Analytical approach of availability and maintainability for structural lifting cables using reliability-based optimization. *Int J Eng Sci* 2012;1(1):21–30.
- [29] López JC, Lavorato M, Rider MJ. Optimal reconfiguration of electrical distribution systems considering reliability indices improvement. *Int J Electr Power Energy Syst* 2016;78(1):837–45.
- [30] Hasanvand S, Nayeripour M, Fallahzade-Abarghouei H. A new distribution power system planning approach for distributed generations with respect to reliability assessment. *J Renew Sustain Energy* 2016; 8(1). <http://dx.doi.org/10.1063/1.4955111>.
- [31] Shahirinia AH, Hajizadeh A, Yu DC, Feliachi A. Control of a hybrid wind turbine/battery energy storage power generation system considering statistical wind characteristics. *J Renew Sustain Energy* 2012; 4(1). <http://dx.doi.org/10.1063/1.4751472>.
- [32] Boyle G. Renewable energy. Oxford, U.K.: Oxford Univ. Press; 2004.
- [33] Nikmehr N, Ravadanegh SN. Reliability evaluation of multi-microgrids considering optimal operation of small scale energy zones under load-generation uncertainties. *Int J Electr Power Energy Syst* 2016;78(1):80–7.
- [34] Bagheri A, Monsef H, Lesani H. Integrated distribution network expansion planning incorporating distributed generation considering uncertainties, reliability, and operational conditions. *Int J Electr Power Energy Syst* 2015;73(1):56–70.
- [35] Zeng B, Zhang J, Ouyang S, Yang X, Dong J, Zeng M. Two-stage combinatory planning method for efficient wind power integration in smart distribution systems considering uncertainties. *Electr Power Compon Syst* 2014;42(15):1661–72.
- [36] Billinton R, Bagen, Cui Y. Reliability evaluation of small standalone wind energy conversion systems using a time series simulation model. *Proc Inst Elect Eng, Gen, Trans, Distrib* 2003; 150: 96–100.
- [37] Rajabi-Ghahnavieh A, Nowdeh SA. Optimal PV–FC hybrid system operation considering reliability. *Int J Electr Power Energy Syst* 2014;60(1):325–33.
- [38] Gorjian S, Hashjin TT, Ghobadian B. Estimation of mean monthly and hourly global solar radiation on surfaces tracking the sun: case study: Tehran. In: Renewable energy and distributed generation (ICREDG), 2012 second iranian conference on; 6–8 March 2012. p. 172–7.
- [39] Liu J, Fang W, Yang Y, Yang C, Lei S, Fu S. Increasing wind power penetration level based on hybrid wind and photovoltaic generation. In: TENCON 2013–2013 IEEE region 10 conference (31194); 22–25 Oct. 2013. p. 1–5.
- [40] Grahm P, Alvehag K, Soder L. PHEV utilization model considering type-of-trip and recharging flexibility. *IEEE Trans Smart Grid* 2014;5(1):139–48.
- [41] Hamzeh M, Hashemi-Dezaki H, Askarian-Abyaneh H, Gharepetian GB, Vahidi B. Risk management of smart grids based on plug-in hybrid electric vehicles' charging considering transformers' hottest spot temperature-dependent aging failures. *J Renew Sustain Energy* 2016; 8(3). <http://dx.doi.org/10.1063/1.4948929>.
- [42] Hashemi-Dezaki H, Hamzeh M, Askarian-Abyaneh H, Haeri-Khiavi H. Risk management of smart grids based on managed charging of PHEVs and vehicle-to-grid strategy using Monte Carlo simulation. *Energy Convers Manage* 2015;100(1):262–76.
- [43] Hamzeh M, Vahidi B, Askarian-Abyaneh H. Reliability evaluation of distribution transformers with high penetration of distributed generation. *Int J Electr Power Energy Syst* 2015;73(1):163–9.
- [44] IEEE reliability test system—a report prepared by the reliability test system task force of the application of probability methods subcommittee. *IEEE Trans Power App Syst* 1979; PAS-98: 2047–54.
- [45] Xu NZ, Chung CY. Well-being analysis of generating systems considering electric vehicle charging. *IEEE Trans Power Syst* PP(99): 1–10. <http://dx.doi.org/10.1109/TPWRS.2014.2307865>.
- [46] Kumar D, Samantaryay SR, Kamw I, Sahoo NC. Reliability-constrained based optimal placement and sizing of multiple distributed generators in power distribution network using cat swarm optimization. *Electr Power Compon Syst* 2014;42(2):149–64.
- [47] Arefifar SA, Mohamed YAI, El-Fouly THM. Supply-adequacy-based optimal construction of microgrids in smart distribution systems. *IEEE Trans Smart Grid* 2012;3(3):1491–502.
- [48] Arefifar SA, Mohamed YAI, El-Fouly THM. Optimized multiple microgrid-based clustering of active distribution systems considering communication and control requirements. *IEEE Trans Ind Electron* 2015;62(2):711–23.
- [49] Delavaripour H, Dehkordi BM. Reliability evaluation of a standalone wind-photovoltaic/battery energy system based on realistic model of battery. *J Renew Sustain Energy* 2015; 7(1). <http://dx.doi.org/10.1063/1.4906772>.
- [50] Wang C. Modeling and control of a hybrid wind/photovoltaic/fuel cell distributed generation systems [Doctor of Philosophy Dissertation]. Bozeman (Montana, USA): Dept. Elect. Eng., Montana State University; 2006.
- [51] Roos F, Lindah S. Distribution system component failure rates and repair times—an overview. In: Proc distribution and asset management conf, Helsinki, Finland; Aug. 2004.
- [52] Nemry F, Leduc G, Muñoz A. Plug-in hybrid and battery electric vehicles: state of the research and development and comparative analysis of energy and cost efficiency. *JRC Technical Notes*; 2009.